

AD-A167 058

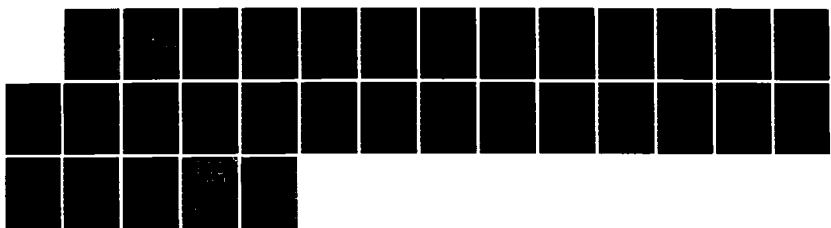
CERENKOV RADIATION AND ELECTROMAGNETIC PULSE PRODUCED
BY ELECTRON BEAMS T. (U) NAVAL POSTGRADUATE SCHOOL
MONTEREY CA F R BUSKIRK ET AL. MAR 86 NPS-61-86-011

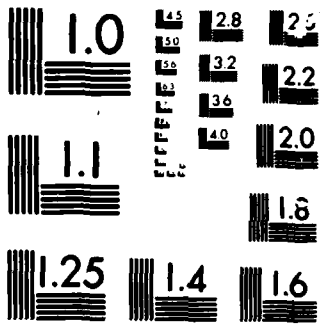
1/1

UNCLASSIFIED

F/G 26/8

NL





MICROCOM[®]

CHART

AD-A167 058

NPS-61-86-011

NAVAL POSTGRADUATE SCHOOL
Monterey, California



DTIC
ELECTED
APR 21 1986

A

CERENKOV RADIATION AND ELECTROMAGNETIC PULSE
PRODUCED BY ELECTRON BEAMS TRAVERSING A
FINITE PATH IN AIR

by

F. R. Buskirk and J. R. Neighbours

March 1986

DTIC FILE COPY

Approved for public release; distribution unlimited

Prepared for: Naval Sea Systems Command
Washington, D.C. 20362

86 4 21 057

NAVAL POSTGRADUATE SCHOOL
Monterey, California

Commodore R. H. Shumaker
Superintendent

D. A. Shrady
Provost

The work reported herein was supported in part by Naval Sea Systems Command, Washington, D.C.

Reproduction of all or part of this report is authorized.

This report was prepared by:

F. R. Buskirk
F. R. BUSKIRK
Professor of Physics

J. R. Neighbours
J. R. Neighbours
Professor of Physics

Approved by:

G. E. Schacher
G. E. SCHACHER
Chairman, Department of Physics

Released by:

J. M. Dyer
J. M. DYER
Dean of Science and Engineering

UNCLASSIFIED

SECURITY CLASSIFICATION OF THIS PAGE (When Data Entered)

REPORT DOCUMENTATION PAGE		READ INSTRUCTIONS BEFORE COMPLETING FORM
1. REPORT NUMBER NPS-61-86-011	2. GOVT ACCESSION NO.	3. RECIPIENT'S CATALOG NUMBER
4. TITLE (and Subtitle) CERENKOV RADIATION AND ELECTROMAGNETIC PULSE PRODUCED BY ELECTRON BEAMS TRaversing A FINITE PATH IN AIR		5. TYPE OF REPORT & PERIOD COVERED
		6. PERFORMING ORG. REPORT NUMBER
7. AUTHOR(s) F. R. Buskirk and J. R. Neighbours		8. CONTRACT OR GRANT NUMBER(s)
9. PERFORMING ORGANIZATION NAME AND ADDRESS Naval Postgraduate School Monterey, CA 93943		10. PROGRAM ELEMENT, PROJECT, TASK AREA & WORK UNIT NUMBERS 62101N N0002485WR14821
11. CONTROLLING OFFICE NAME AND ADDRESS Naval Postgraduate School Monterey, CA 93943		12. REPORT DATE March 1986
		13. NUMBER OF PAGES
14. MONITORING AGENCY NAME & ADDRESS (if different from Controlling Office) Naval Sea Systems Command Washington, D.C. 20362		15. SECURITY CLASS. (of this report) UNCLASSIFIED
		15a. DECLASSIFICATION DOWNGRADING SCHEDULE
16. DISTRIBUTION STATEMENT (of this Report) Approved for public release, distribution unlimited		
17. DISTRIBUTION STATEMENT (of the abstract entered in Block 20, if different from Report)		
18. SUPPLEMENTARY NOTES		
19. KEY WORDS (Continue on reverse side if necessary and identify by block number) Radiation Radio Frequency Emissions Relativistic Electron Beams Electrons in Air		
20. ABSTRACT (Continue on reverse side if necessary and identify by block number) Coherent Cerenkov radiation has been investigated previously in the time domain for an infinite path. The present calculations for a finite path length show an effect analogous to diffraction (in the frequency domain) in which radiation fields appear both at Cerenkov angles and at other angles. The latter have previously been named electromagnetic pulse fields.		

CERENKOV RADIATION AND ELECTROMAGNETIC PULSE PRODUCED BY
ELECTRON BEAMS TRAVERSING A FINITE PATH IN AIR

by

Fred R. Buskirk

and

John R. Neighbours

Physics Department

Naval Postgraduate School

Monterey, California 93943

and

Hydrodynamics Group

Los Alamos National Laboratory

Los Alamos, NM 87545

ABSTRACT

Coherent Cerenkov radiation has been investigated previously in the time domain for an infinite path. The present calculations for a finite path length show an effect analogous to diffraction (in the frequency domain) in which radiation fields appear both at Cerenkov angles and at other angles. The latter have previously been named electromagnetic pulse fields.



Accession For	
NTIS	CPA&I
DOD	TAB
Uncontrolled	
Classification	
By	
Distribution/	
Availability Codes	
Avail Ind/cr	
Dist	Special
A1	

I. INTRODUCTION

Cerenkov radiation occurs when charge moves faster than radiation in a medium. Most work 1-4 is concerned with optical radiation produced by a point charge, and involves the Fourier spectra of these fields. Here, in contrast, we explore the time dependence of the radiation fields, using our earlier⁵ formulation to describe the radiation from a bunch of electrons passing through an infinite medium; however, now the medium has finite length, which causes diffraction so that the radiation is produced at other angles than the usual Cerenkov angle. This spreading by diffraction was investigated earlier in the Fourier expansion approach,⁶⁻⁸ but using the present time dependent fields, new insights are developed, and for shorter paths, the Cerenkov fields are related to other forms of radiation, namely, what is referred to as electromagnetic pulse (EMP)⁹, transition and ordinary dipole radiation. It is much easier to understand Cerenkov radiation from a finite-size charge than from a point charge; in the former case, the Cerenkov fields remain finite but become singular for a point charge.¹⁰

II. TIME DEPENDENCE OF FIELDS

Let all charges within a bunch move along the z-axis with the same velocity v , which is larger than the velocity c of radiation in the medium. Let c_0 be the velocity of radiation in

vacuum, let $s^2 = x^2 + y^2$, and assume the volume charge density ρ_v has the form

$$\rho_v(\vec{r}, t) = \rho_0(z-vt)\delta(x)\delta(y) \quad (1)$$

where ρ_0 represents an arbitrary line density. Following our earlier work⁵, the vector potential is

$$\vec{A}(\vec{r}, t) = \frac{\vec{v}}{c_0} \int R^{-1} \rho_0(u) dz' \quad (2)$$

where the variable $u = z' - vt'$ becomes

$$u = z' - vt + \frac{v}{c} [s^2 + (z-z')^2]^{1/2} \quad (3)$$

Retardation is included by the form of u in Eq. 3. The magnetic field B has radiation terms resulting from taking the derivatives of ρ_0 in Eq. 2. This leads to B in the θ direction of cylindrical coordinates, with a magnitude

$$B = \frac{v^2}{cc_0} \int \frac{s}{R^2} \rho'_0(u) dz' . \quad (4)$$

An approximate evaluation of Eq. (4) proceeds as follows: $u(z')$ is plotted as a function of z' . For further calculation assume ρ_0 has linear rising and falling ramps, of width a , separated by a distance b . Then ρ_0 consists of two opposite polarity square

pulses. For early times, the u curve is high (see Reference 5, Fig. 1) and the integrand is zero for all values of z' . As time increases, the u curve drops and the minimum intersects the ρ_0 pulse, and contributes to the integral in Eq. (4). The field \vec{E} may also be calculated; in Ref. 5 it was shown that \vec{E} is perpendicular to \vec{B} and to \vec{R}_m , and \vec{R}_m , the vector from the particle (at the retarded time) to the observer, is at an angle of ω_c to the z -axis. Then $E/B = c/c_0$; both the fields fall off as $R^{-1/2}$, appropriate for radiation from a cylindrical source, and the total energy radiated agrees with the Fourier approach. The two opposite pulses of the radiation field have the same separation as the front and rear slopes of the current pulse.

We now calculate the radiation fields for the case of a finite path. The physical situation shown in Fig. 1 is one in which a beam emerges at $z' = 0$ from an accelerator, passes through a dielectric medium and at $z' = Z$, stops in an absorber. The path (usually air) from $z' = 0$ to Z is the radiator. The beam bunch has a linear rising ramp of length a , is then constant and has a linear decrease of length a , with an effective length b , from the midpoint of the rise to the mid point of the fall.

The calculation of the fields is based on Eq. (4) for B ; corresponding results will hold for E . We again assume that s/R^2 is about constant in the range of integration and may be factored out. Then $s/R = \sin \theta$ and we have

$$B = \frac{v^2}{cc_0} \frac{\sin \theta}{R} \int \rho_0'(u) dz' . \quad (5)$$

The main difference between the calculations below and those done previously⁵ is that the range of z' is finite, from 0 to Z , to represent a finite length (Z) of radiation source. The results of the integration depend on the relation of various parameters.

A. Outside the Cerenkov Cone, Z Long

Fig. 2 represents the situation involved in evaluating Eq. (5). The $u(z')$ curve moves down in time (Eq. 3). For early times, the integrand is always zero. Later the u curve moves down and intersects the dotted rectangle representing the region of u and z' where the integrand is constant. In the situation shown, the integral builds up to a peak value in a time interval a/v , and the integral saturates at the value $\rho_0 \Delta z = \rho_0 a/\text{slope}$ of u -curve. From Eq. (3), the slope is

$$\begin{aligned} \frac{\partial u}{\partial z'} &= 1 - \frac{v}{c} \frac{z - z'}{\sqrt{s^2 + (z - z')^2}} \\ &= 1 - \frac{v}{c} \cos \theta . \end{aligned} \quad (6)$$

Furthermore $\rho_0 a$ is the peak value of ρ_0 which is $I_0 c_0 / v$, where I_0 is the peak current.

Thus the integral saturates at

$$B_{\max} = \frac{v}{c} \frac{\sin \theta}{R} I_0 \frac{1}{1 - \frac{v}{c} \cos \theta} \quad (7)$$

where R is measured from the start of the source, $z' = 0$, to the observer, and it makes an angle θ to the z-axis.

The rise time was a/v , a similar fall time occurs, and the duration of the pulse is given by $Z(\text{slope of } u \text{ curve})/v$ or $Z(1 - \frac{v}{c} \cos \theta)/v$. Because this combination appears often, we define the effective length

$$Z_e = Z(1 - \frac{v}{c} \cos \theta) \quad (8)$$

The significance of Z_e is that it yields the time difference for two signals emitted by a given charge at two points separated by a distance Z in the lab. Note that $Z_e = 0$ at the Cerenkov angle, as expected, because signals emitted at θ_c from all parts of the path reach a distant observer at the same time.

Thus we have, for the leading ramp of the current pulse, a field at the observer of value given by Eq. (7) with lengths shown in Fig. 3a. Here the lengths are times multiplied by v. Also shown is the negative field pulse caused by the back ramp of the current pulse. The two pulses combine to give the symmetric pulse of Fig. 3b, with a separation that is the larger of Z_e or b , and a duration that is the smaller of Z_e or b .

B. On the Cerenkov Cone

If the observer is in the Cerenkov region (region B in Fig. 1), the rectangular region of integration in Fig. 1 is centered about the minimum in the $u(z')$ curve. If Z is large, the integral for the field is the same as in our earlier paper. The pulse starts when the $u(z')$ curve, as it advances down in time, becomes tangent to the rectangular integration region. The integral increases as $t^{1/2}$ until the u curve is tangent to the lower boundary, and then decreases, again proportional to $t^{1/2}$. The result is

$$B_{\max} = \frac{v^2}{c^2} \frac{1}{R_m} \frac{\sin \theta_c}{\tan^{3/2} \theta_c} I_0 \frac{2\sqrt{Z}}{\sqrt{s/a}} \quad (9)$$

The positive and negative pulses have rise and fall times of a/v and are separated by b/v . The field falls as $1/R_m$ as one proceeds outward at a fixed angle with $s = R_m \sin \theta_c$.

If the path is short, the B field pulse, as a function of time, increases as $t^{1/2}$ as noted above, but the maximum value of the integral for Eq. (5) occurs when the $u(z')$ curve first intersects the vertical limits (0 and Z) of integration of the rectangular region in the $u-z'$ plane. Then the maximum magnetic field becomes

$$\begin{aligned} B_{\max} &= \frac{v^2}{cc_0} \frac{\sin \theta_c}{R_m} \rho'_0 (u) Z \\ &= \frac{v^2}{cc_0} \frac{\sin \theta_c}{R_m} \rho'_0 a + \frac{Z}{a} . \end{aligned} \quad (10)$$

Eliminating ρ_0 in terms of I_0 yields:

$$B_{\max} = \frac{v}{c} \frac{\sin \theta_c}{R_m} I_0 \frac{z}{a} . \quad (11)$$

In this case, positive and negative pulses of width a have a separation b , which is the same as for the long radiator, but the pulses have flat tops.

If the observer moves out along the Cerenkov cone, the long path case changes into the short path case. In the former, the source is long and the observer sees a field associated with cylindrical symmetry. But as the observer moves out, the radiator of length Z appears to be short, leading to the R^{-1} field of Eq. (10) instead of the R^{-1} (cylindrical) field of Eq. (9). The transition from the cylindrical wave to the spherical wave occurs when $2\Delta z$ (defined in Eq. (18) of Ref. 5) is equal to Z . This yields for the value of s , denoted by s_s

$$a s_s \frac{v^2}{c^2} \frac{2}{\tan^3 \theta_c} = Z^2 . \quad (12)$$

That is, for $s > s_s$ [where s_s satisfied Eq. (12)] the wave becomes spherical and decreases as R^{-1} or s^{-1} .

C. Outside the Cerenkov Cone, Z Short

In the previous sections, cases were considered in which $Z_e > b > a$, but other situations are possible. Because a is the rise

and fall length of the current pulse, and b is the width measured between the half-maximum points, we must have $b \geq a$. We could then have $b > z_e > a$ and $b > a > z_e$ cases. For the latter the field is again obtained by evaluating Eq. (5). The horizontal range of integration is short so that the range of the variable z' is always Z , if we are off the Cerenkov cone. The result is

$$B = \frac{v^2}{cc_0} \frac{\sin \theta}{R} \rho_0 z . \quad (13)$$

Noting that $\frac{v}{c_0} \rho_0 a = I_0$, the peak current in the pulse, we find

$$B = \frac{v}{c} \frac{\sin \theta}{R} I_0 \frac{z}{a} . \quad (14)$$

The field pulse at the observer will have a rise and fall time z_e/v , the pulse length is a/v , and it will be followed by a similar negative pulse at a time b/v later.

III. SEMI-INFINITE PATH

Let the beam emerge from the accelerator window at $z = 0$ and traverse a path, which is idealized to be infinitely long. Starting from the point where the beam emerges, define a cone with apex angle θ_c relative to the beam. If the observer is anywhere inside the cone, the minimum of the $u(z')$ curve will

intersect the $\rho_0(u)$ pulses, and the radiation field will be the same as found in Ref. 5 and described in Sec. II. B. The radiation fields will have a positive and negative pulse separated by a distance b . This region is dominated by Cerenkov radiation.

Now let the observer be outside the Cerenkov cone. The situation is somewhat like that described in Sec. II., except that the horizontal range of integration is infinite in the positive direction. The rising part, or head, of the current pulse leads to fields which are essentially constant, whereas the following tail gives an opposite field delayed by a time b/v . We thus have a field pulse in the region outside the Cerenkov cone of length b but only of one sign. This is EMP, and in the above model, both EMP and Cerenkov radiation exist. The field lines are shown qualitatively in Fig. 4.

IV. JUSTIFICATION OF MODEL

The model using a finite path is supposed to represent radiation from a bunch of electrons, emerging from an accelerator system at $z' = 0$, and stopped by some means at $z' = Z$. No specific account has been made for these boundaries; radiation by return currents has been neglected. Consider the following model: the charge that suddenly appears at $z' = 0$ in all the cases is furnished by a source electron pulse of lower velocity v_s which moves in the region $z' < 0$ and meets the previously specified pulse at $z' = 0$. To conserve charge at all times at $z' = 0$, $b_s = b \frac{v_s}{v}$, $a_s = a \frac{v_s}{v}$ and $I_{os} = I_o$, where I_{os} , a_s , and b_s

are the current, rise, and width parameters for the slow pulse approaching the boundary from negative z' .

The radiation pulse from the slow incoming electrons is given by Eq. (7) with the appropriate lower velocity v_s substituted. By inserting a very low value of v_s the field becomes small, and because b_s becomes small, the time in which the field pulse occurs becomes short, so that the radiated energy becomes very small. Thus we conclude that inclusion of source and return currents, required to conserve charge, contribute little to radiation fields calculated, and may be neglected.

V. DISCUSSION

Cerenkov radiation has been described above and in Ref. 5 in terms of time dependence of the radiation fields caused by finite charge distributions such as are realized by bunches emitted by an accelerator. In the usual Fourier-expansion formalism, either a finite size of the charge or dispersion in the medium limits the radiated power at the high-frequency end of the spectrum, and a finite length of path in the medium produces diffraction of the angle of the emitted radiation about the Cerenkov angle.

The present time-dependent field formulation reveals the following properties of Cerenkov radiation: A. The radiation is associated with dI/dt at the leading and trailing parts of the pulse. B. The Cerenkov radiation (for an infinite path) consists of positive and negative pulses separated by a distance, which is the pulse length. C. For a semi-infinite path, Cerenkov radiation appears within a cone of angle θ_C , whose apex

is at the start of the path. An EMP pulse appears outside that cone. D. For a finite path of length Z, both Cerenkov and EMP appear, the latter dominating as Z becomes smaller. For Z short and β small, the $\sin \theta / (1 - \beta \cos \theta)$ dependence of the EMP pulse becomes $\sin \theta$; thus the fields at low β becomes essentially a single pulse of dipole radiation.

Finally it should be noted that Cerenkov radiation is not a different radiation to be added on to other forms of radiation when $v > c$ (medium) but should appear naturally in a correct calculation of the radiation. If $v < c$, radiation also occurs but without the characteristic shockwave-like character of Cerenkov radiation.

ACKNOWLEDGMENT

We gratefully acknowledge the support of the Hydrodynamics Group, Los Alamos National Laboratory, for Fred R. Buskirk during the period from July 1984 to July 1985. We also acknowledge the support of the U.S. Naval Sea Systems Command.

REFERENCES

1. J. V. Jelley, "Cerenkov Radiation and Its Applications," (Pergamon, London, 1958).
2. V. P. Zrelov, "Cerenkov Radiation in High Frequency Physics," (Atomizdat, Moscow, (1968); translation: Israel Program for Scientific Translations, Jerusalem, (1970)).
3. B. M. Bolotovskii, Usp. Fiz. Nauk LXII, 201 (1957).
4. M. Phillips, "Classical Electrodynamics," in Encyclopedia of Physics, Vol IV, Ed. by S. Fluggeee, Springer (1962).
5. F. R. Buskirk and J. N. Neighbours, Phys. Rev. A 31 3750 (1985)
6. F. R. Buskirk and J. R. Neighbours, Phys. Rev. A 28, 1531 (1983).
7. J. R. Neighbours and F. R. Buskirk, Phys. Rev. A 29, 3246 (1984).
8. A. P. Kobzev, Yad. Fiz. 27, 1256 (1978) [Sov. J. Nucl. Phys. 27, 664 (1978)]; A. P. Kobzev and I. M. Frank, ibid. 31, 1253 (1981) [34, 71 (1981)].

9. T. A. Tumolillo, J. P. Wondra, W. E. Hobbs, and K. Smith,
IEEE Trans. Nucl. Sci. NS27 1951 (1980).

10. I. Tamm, J. Phys. SSSR 1 439 (1939).

FIGURE CAPTIONS

Fig. 1. For a finite path length Z , an observer in regions A or C finds EMP radiation, shown in Fig. 4 and developed in Secs. II.A and II.C. In region B, a Cerenkov field pulse described in Sec. II.B occurs.

Fig. 2. The variable u plotted as a function of z' . As time increases, the curves are displaced downward. The derivative of the current pulse is shown. When the $u(z')$ first intersects the ρ_0 pulse, the integrand of Eq. (4) becomes nonzero, and the Cerenkov pulse starts (Sec. II).

Fig. 3. The field pulse outside the Cerenkov cone for finite path length. Curve (a) shows the positive and negative pulses separately, whereas (b) shows the composite field. The separation S is the larger of Z_e or b , whereas the duration D is the smaller (Sec. II.A and II.C.)

Fig. 4. A qualitative representation of field lines for an electron bunch traversing a semi-infinite path. As the position of the observe changes, the pulse form changes as shown in the inset. Cerenkov radiation occurs at the lower right; EMP pulses occur to the upper left.

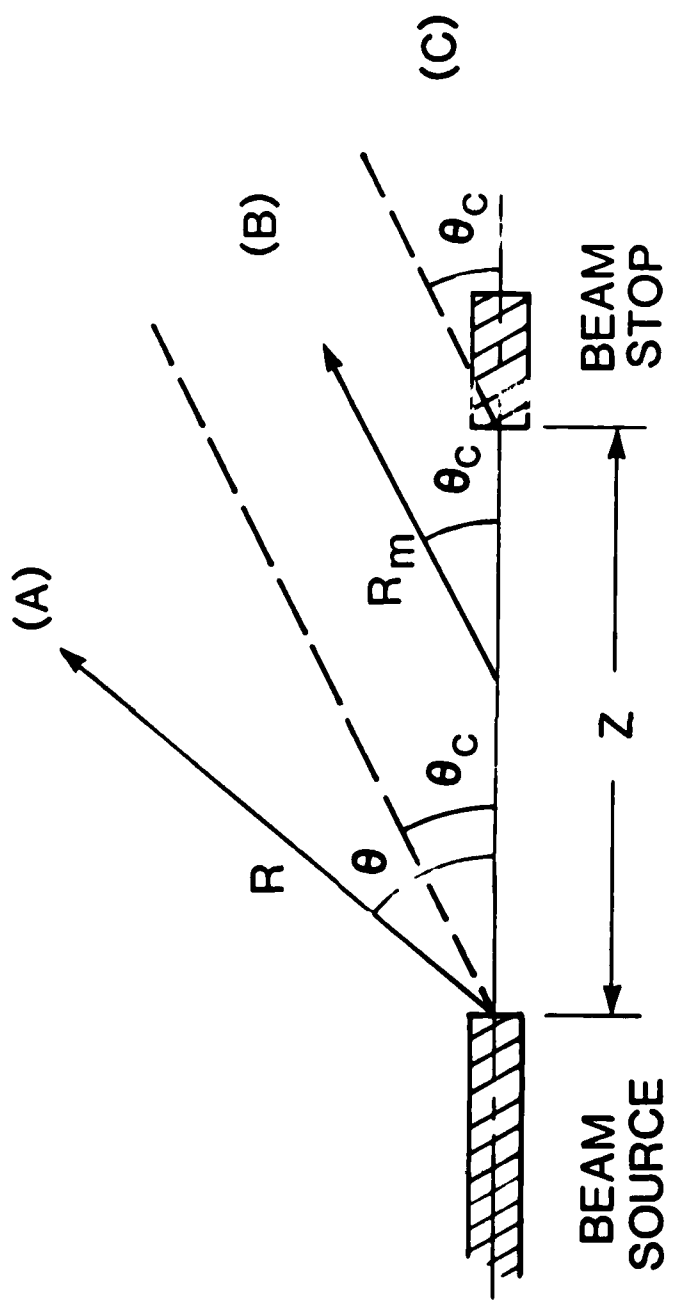


Figure 1

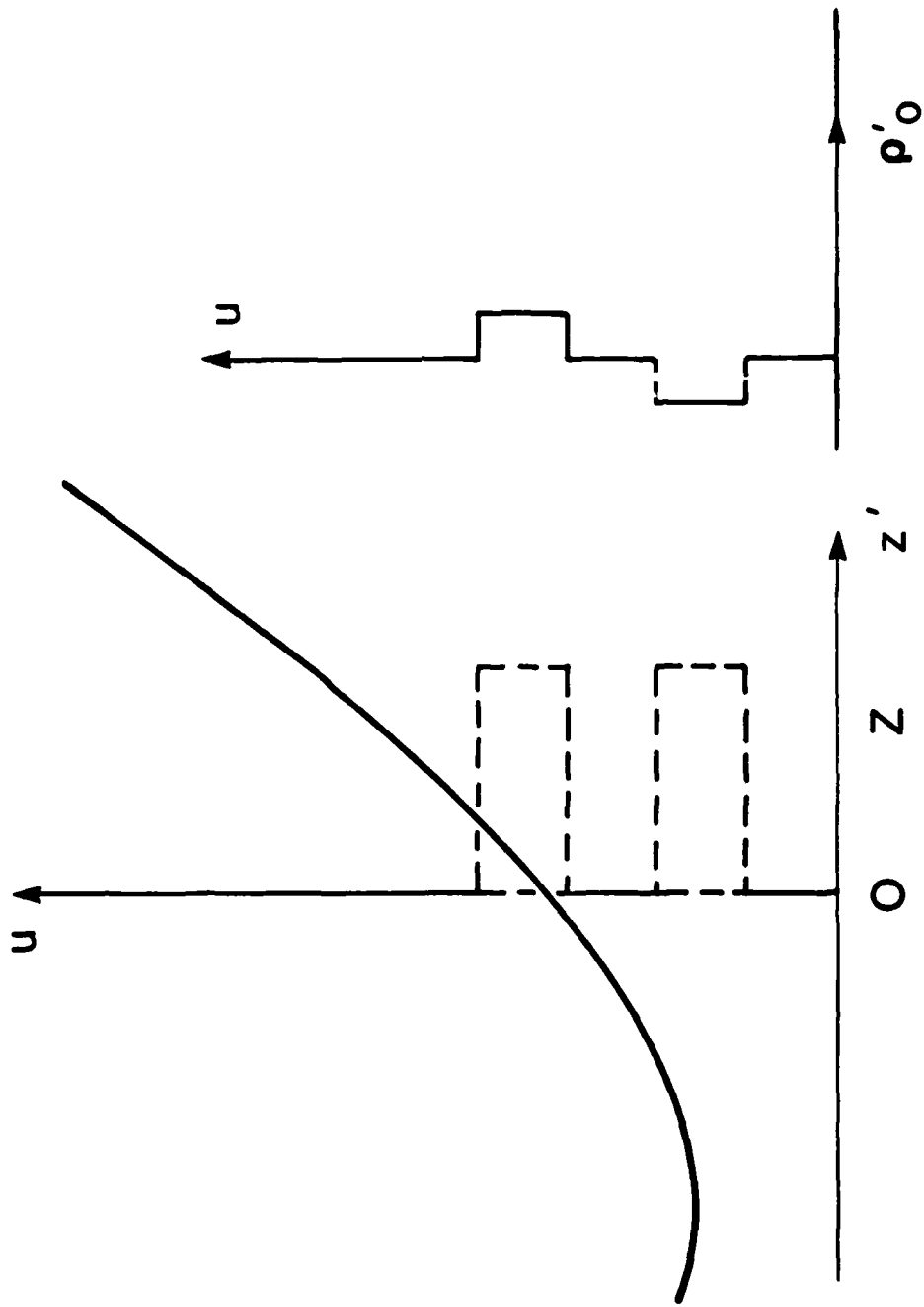


Figure 2

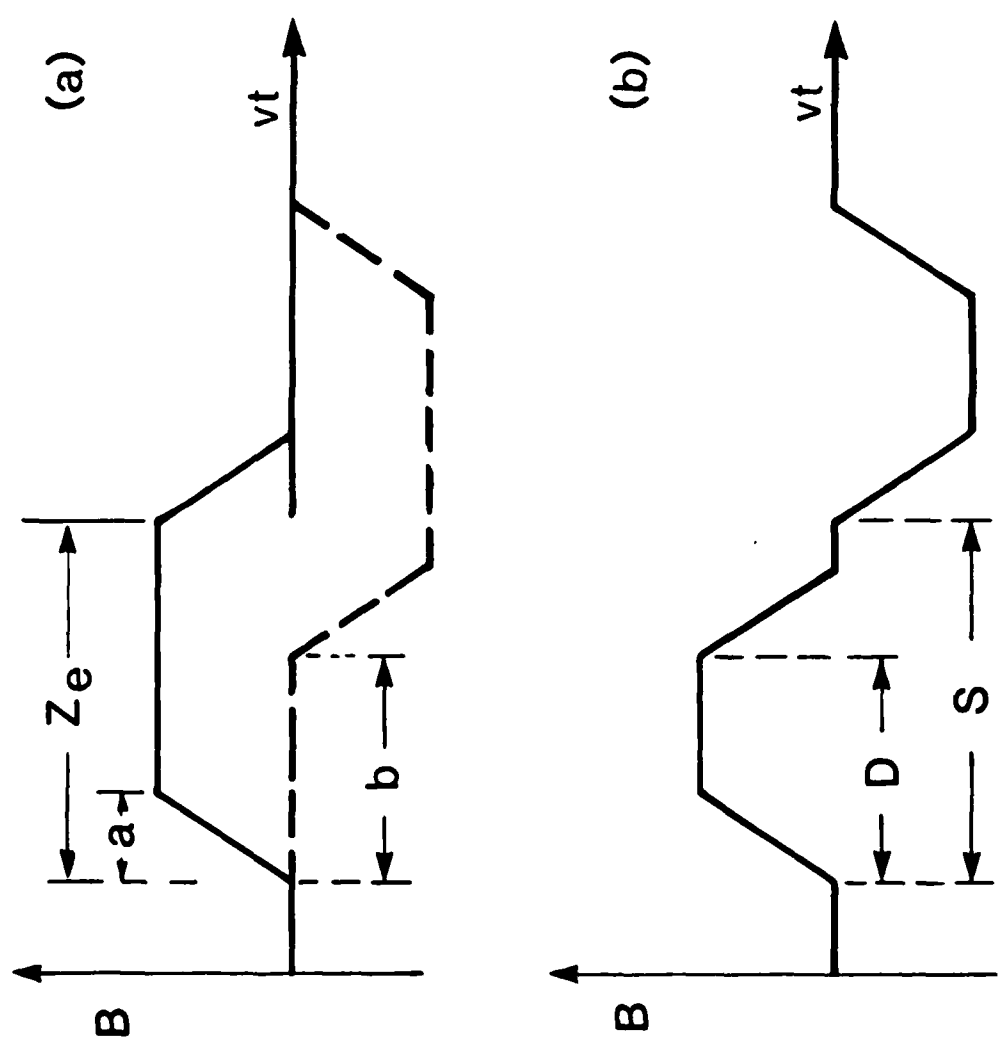


Figure 3

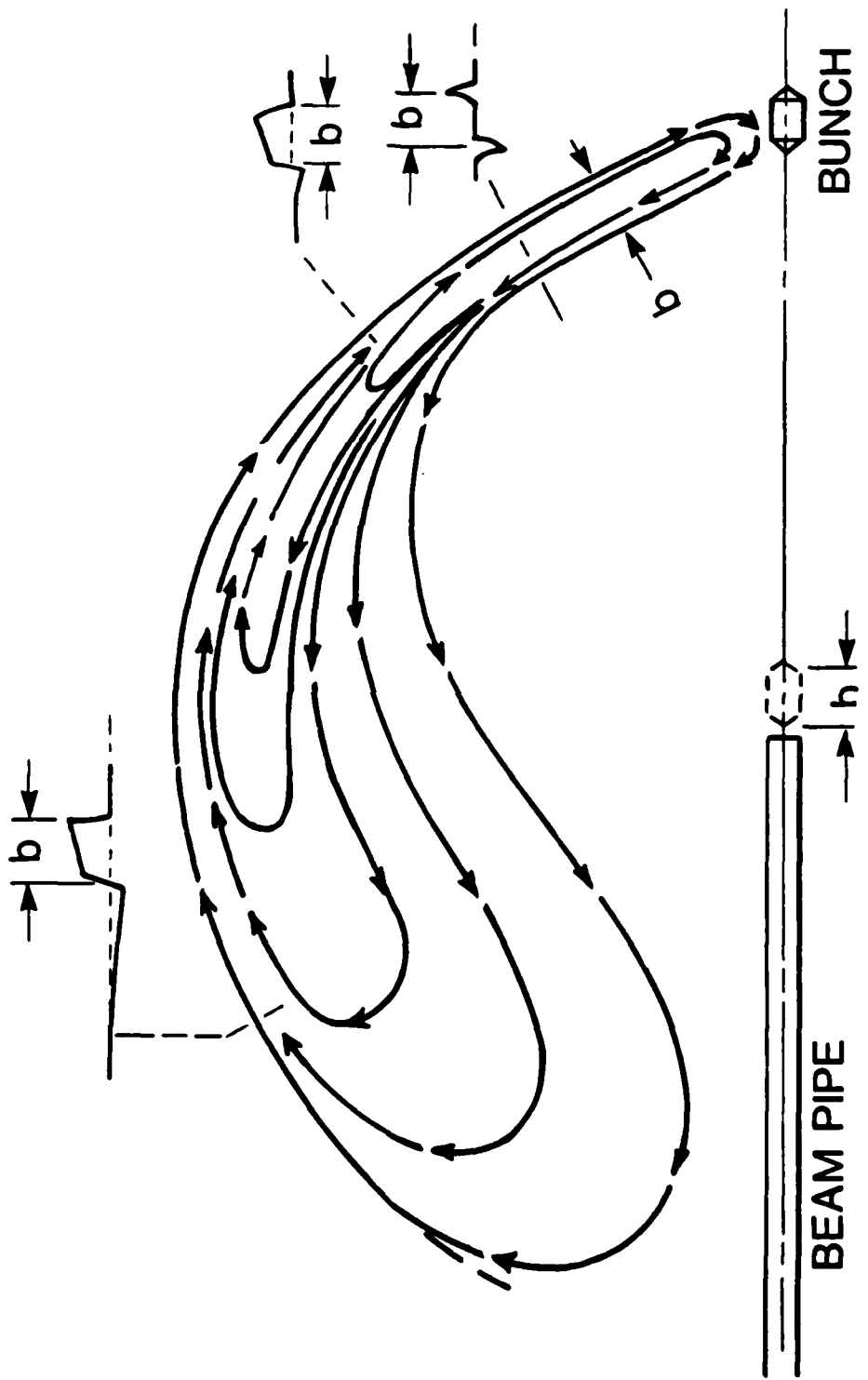


Figure 4

DISTRIBUTION LIST

CDR William Bassett PMS 405 Strategic Systems Project Office Naval Sea Systems Command Washington, D.C. 20376	1
Dr. H. Boehmer TRW One Space Park Redondo Beach, CA 92078	1
Dr. Richard Briggs L-321 Lawrence Livermore National Laboratory Box 808 Livermore, CA 94550	2
F. R. Buskirk & J. R. Neighbours Naval Postgraduate School Physics Department, Code 61 Monterey, CA 93943	20
Prof. C. D. Cantrell Department of Physics University of Physics University of Texas at Dallas P. O. Box 688 Richardson, TX 75080	1
The Charles Stark Draper Laboratory Attn: Dr. Edwin Olsson 555 Technology Square Cambridge, MA 02139	1
Dr. A. N. Chester Hughes Research Laboratories 3011 Malibu, CA 92065	1
Dr. W. Colson Berkeley Research Associates P. O. Box 241 Berkeley, CA 94701	1
Director, Defense Advanced Research Project Agency ATTN: LCOL Richard A. Gullickson 1400 Wilson Blvd. Arlington, CA 22209	2

Defense Advanced Research Project Agency ATTN: MAJ George P. Lasche 1400 Wilson Blvd. Arlington, VA 22209	1
Defense Advanced Research Projects Agency Attn: Dr. Shen Shey Directed Energy Office 1400 Wilson Boulevard Arlington, VA 22209-2308	1
Defense Technical Information Center Cameron Station Alexandria, VA 22314	2
Directed Technologies Attn: Mr. Ira F. Kuhn, Jr. Dr. Nancy J. Chesser 1226 Potomac School Road McLean, VA 22101	2
Dr. J. Eckstein Hansen Laboratory Stanford University Stanford, CA 94305	1
Dr. Luis Elias Physics Department UCSB Santa Barbara, CA 93106	1
Dr. K. Felch Varian Corporation 611 Hansen Way Palo Alto, CA 94303	1
Dr. V. L. Granatstein Electrical Engineering Dept. University of Maryland College Park, MD 20742	1
Dr. C. M. Huddleston ORI, Inc. 1375 Piccard Drive Rockville, MD 20850	1
Prof. N. Kroll Physics Department UCSD San Diego, CA 92037	1

La Jolla Institute
Attn: Dr. K. Brueckner
P. O. Box 1434
La Jolla, CA 92038

1

Lawrence Berkeley Laboratory
Attn: Dr. Edward P. Lee
Building 47, Room 111
1 Cyclotron Road
Berkeley, CA 94720

1

Lawrence Livermore National Laboratory
Univeristy of California
Attn: Dr. William A. Barletta
Dr. Daniel S. Prono
Dr. Adrian C. Smith
Dr. Simon S. Yu
Dr. John T. Weir
Dr. Thomas J. Karr
Dr. William M. Fawley
Dr. Eugene J. Lauer
Dr. George J. Caporaso
Ms. Lois Barber
P. O. Box 808
Livermore, CA 94550

10

Library
Code 0142
Naval Postgraduate School
Monterey, CA 93943

2

Lockheed Missile and Space Co., Inc.
Attn: Dr. John Siambis
P. O. Box 3504
Sunnyvale, CA 94088-3504

1

Los Alamos National Laboratory
Attn: Dr. Randolph Carlson
Dr. S. Szuchlewski
Dr. J. M. Mack
Ms. Leah Baker
Mail Stop P942
P. O. Box 1663
Los Alamos, NM 87545

4

Dr. Joseph Mack
M4, M.S. P-940
Los Alamos National Laboratory
Los Alamos, NM 87545

1

Dr. J. Madey Department of Physics Stanford University Stanford, CA 94305	1
Prof. T. C. Marshall Dept. of Applied Physics and Nuclear Engineering Columbia University New York, NY 10027	1
Dr. Xavier K. Maruyama Bldg. 245, Room R-108 National Bureau of Standards Gaithersburg, MD 20899	1
McDonnell-Douglas Corp. Attn: Dr. J. Carl Leader P. O. Box 516 St. Louis, MS 63166	1
Dr. David Merritt PMS 405 Strategic Systems Project Office Naval Sea Systems Command Washington, D.C. 20376	1
Mission Research Corporation Attn: Dr. N. J. Carron P. O. Box 719 Santa Barbara, CA 93102	1
Mission Research Corporation Attn: Dr. Brendan B. Godfrey Dr. Larry Wright Dr. Barry Newberger Dr. R. Adler Dr. G. Kiuttu Dr. T. Hughes Dr. Dushan Mitrovitch Plasma Sciences Division 1720 Randolph Road, SE Albuquerque, NM 87106	7
Prof. G. T. Moore University of New Mexico Department of Physics 800 Yale Boulevard N.E. Albuquerque, NM 87131	1

Naval Research Laboratory 10
Attn: Dr. Martin Lampe (4790)
Dr. J. Robert Greig (4763)
Dr. Richard Hubbard (4790)
Dr. A. Wahab Ali (4700.1)
Dr. Robert Pechacek (4760)
Dr. Donald Murphy (4760)
Dr. Richard Fernsler (4770)
Dr. Bertrum Hui (4790)
Dr. Glen Joyce (4790)
Ms. Wilma Brizzi (4790)
4555 Overlook Avenue, SW
Washington, DC 20375

Naval Surface Weapons Center 9
White Oak Laboratory
Attn: Dr. Eugene E. Nolting (R401)
Dr. Andy Smith (H23)
Ms. Beverly McLean (R401)
Dr. H. C. Chen (R41)
Dr. Han S. Uhm (R41)
Dr. Ralph Fiorito (R41)
Dr. John Smith (R41)
Dr. Donald Rule (R41)
Dr. M. J. Rhee (R41)
10901 New Hampshire Avenue
Silver Springs, MD 20903-5000

Office of Naval Research 1
CDR James Offutt
1030 East Green Street
Pasadena, CA 91106

Office of Naval Research 1
CDR R. Swafford
800 N. Quincy Street
Arlington, VA 22217

Office of Research Administration 1
Code 012
Naval Postgraduate School
Monterey, CA 93943

Dr. C. Pellegrini 1
Brookhaven National Laboratory
Bldg 902
Accelerator Dept.
Upton, NY 11973

MAJ E. W. Pogue 1
M4, M.S. P-940
Los Alamos National Laboratory
Los Alamos, NM 87545

Sandia National Laboratory Attn: Dr. Michael Mazarakis (1272) P. O. Box 5800 Albuquerque, NM 87185	1
Sandia National Laboratories Attn: Dr. Carl Ekdahl (1272) Dr. Ron Lipinski Dr. Michael Mazarakis (1272) Dr. John Freeman (1241) Dr. Gordon T. Leifeste (1272) P. O. Box 5800 Albuquerque, NM 87185	5
Science Applications International Corp. Attn: Dr. Robert Johnston Dr. R. Leon Feinstein Dr. R. Richardson Dr. Douglas Keeley Dr. C. Yee 5150 El Camino Real, Suite B-31 Los Altos, CA 94022	5
SRI International Attn: Dr. Donald J. Eckstrom 333 Ravenswood Avenue Menlo Park, CA 94025	1
CAPT Kurt Stevens AFTAC/TX OP Patrick AFB Patrick, FL 32925	1
Strategic Defense Initiative Organization Directed Energy Weapons Office The Pentagon Attn: LTCOL Richard L. Gullickson Office of the Secretary of Defense Washington, D.C. 20301-7100	1
Dr. Kenneth W. Struve Lawrence Livermore National Laboratory P. O. Box 808 Livermore, CA 94550	1
Dr. A. Szoke L-71 LLL Livermore, CA 94550	1

Admiral R. L. Topping Space and Naval Warfare Systems Command SPAWAR-06 Washington, D.C. 20363-5100	1
LCDR E. Turner PMS 405 Strategic Systems Project Office Naval Sea Systems Command Washington, D.C. 20376	1
Dr. R. Warren Los Alamos Scientific Laboratory P. O. Box 1663 Los Alamos, NM 87545	1
Prof. G. J. Yevick Physics Department Stevens Institute of Technology Castle Point Station Hoboken, NJ 07030	1
Naval Sea Systems Command Washington, D.C. 20362	2

END

FILMED

5-86

DTIC

